Dislocation dynamics and crystal plasticity in the phase field crystal model

Audun Skaugen* and Luiza Angheluta
Department of Physics, University of Oslo, P.O. Box 1048 Blindern, N-0316 Oslo, Norway

Jorge Viñals
School of Physics and Astronomy, University of Minnesota, 116 Church St. SE, Minneapolis, MN 55455, USA

A phase field model of a crystalline material is introduced to develop the necessary theoretical framework to study plastic flow due to dislocation motion. We first obtain the elastic stress from the phase field crystal free energy under weak distortion, and show that it obeys the stress strain relation of linear elasticity. We focus next on dislocations in a two dimensional hexagonal lattice. They are composite topological defects in the weakly nonlinear amplitude equation expansion of the phase field, with topological charges given by the standard Burgers vector. This allows us to introduce a formal relation between dislocation velocity and the evolution of the slowly varying amplitudes of the phase field. Standard dissipative dynamics of the phase field crystal model is shown to determine the velocity of the dislocations. When the amplitude expansion is valid and under additional simplifications, we obtain that the dislocation velocity is determined by the Peach-Koehler force. As an application, we compute the defect velocity for a dislocation dipole in two setups, pure glide and pure climb, and compare it the analytical predictions.

PACS numbers: 46.05.+b,61.72.Bb,61.72.Lk,62.20.F-

I. INTRODUCTION

The description of plastic response in crystals at a mesoscale level poses fundamental challenges because of collective effects in dislocation dynamics that give rise to multiple-scale phenomena, such as spatio-temporal dislocation patterning [1, 2] and intermittent deformations [3]. Different multiscale models including discrete dislocation models, stochastic models, and cellular automata have been proposed and used to explore various aspects of collective dislocation dynamics [4–6]. We focus here on a phase field description of a crystalline solid, the so-called phase field crystal, first introduced by Grant and collaborators [7–9]. This model has allowed the study of defect configurations and their kinetics that are difficult to address with either microscopic or atomistic simulation techniques, or with classical continuum mechanics. Examples include large strain formulations of dislocation motion [10], creep motion mediated by diffusion [11], or defect core transformations that are seen to be key to the motion of grain boundaries [12].

A mesoscale theory is also timely given that defect imaging techniques are beginning to reveal strain and rotation fields created by one or a small number of defects in atomic detail. High Energy Diffraction Microscopy and Bragg Coherent Diffractive Imaging represent the state of the art in imaging at advanced synchrotron facilities [13, 14]. The former can provide three dimensional maps of grain orientations with micron resolution, whereas the latter can determine atomic scale displacements with $\leq$ 30 nm resolution. Advanced image processing methods allow the determination of the strain field phase around a single defect, clearly evidencing its multivalued nature. Indeed, single dislocations have been successfully imaged and their motion tracked quantitatively just recently [15]. Experiments also go beyond the determination of strain fields, and determine other quantities sensitive to the topology of the defects. For example, lattice rotation has been imaged and analyzed in nanoindentation experiments [16], or in two dimensional graphene sheets [17].

Mesoscale models aim at bridging fully atomistic descriptions and macroscopic theory based on continuum mechanics. Along these lines, we mention the so called generalized disclination theory [18, 19]. This theory is a fully resolved nano scale yet continuum dynamical description of dislocations that preserves all topological constraints necessary in the kinematic evolution of the singular fields. Singularities are replaced by topologically equivalent but smooth local fields that allow a full derivation of the governing dynamical equations following the principles of irreversible thermodynamics. The newly introduced fields are similar to a phase field model, except that they are constructed to satisfy all conservation laws, including those of topological origin. On the other hand, the dynamical part of the theory requires constitutive input for both the free energy at the mesoscale, functional of the smooth fields, and mobility relations for their motion.

Conventional phase field models have also become one of the tools of choice in the study of dislocation and grain boundary motion in a wide variety of circumstances. Contrary to kinematic models, a phenomenological set of dynamical laws for the phase field are introduced, with topological invariants appearing as derived quantities. There are two different classes of phase field models

*audun.skaugen@fys.uio.no

in the plasticity literature. In one approach, the elementary dislocation is described as an eigenstrain, which is then mapped onto a set of phase fields [20–22]. If **b** is the Burger's vector of the dislocation, and **n** the normal to the dislocation line, then the corresponding eigenstrain is defined as

$$u^*_{ij} = \frac{b_i n_j + b_j n_i}{2a} \tag{1}$$

where a is the crystal lattice spacing. The connection to the phase fields $\phi_\alpha(\mathbf{x})$, where α label all the slip systems of a particular lattice, is made through the decomposition

$$u^*_{ij} = \sum_\alpha \epsilon^{*\alpha}_{ij} \phi_\alpha(\mathbf{r}). \tag{2}$$

The phase fields are assumed to relax according to purely dissipative dynamics driven by minimization of a phenomenological free energy. This free energy includes a non-convex Ginzburg-Landau type contribution of the same functional form as related studies in fluids [23]. This contribution is supplemented by an elastic interaction energy that depends only on the incompatibility fields associated with the eigenstrains [24–26], and hence, ultimately, on the phase fields themselves [20–22].

The second approach, which we adopt here, is based on a physical interpretation of the phase field as a temporally coarse-grained representation of the molecular density in the crystalline phase. Such as model is also known as the phase field crystal (PFC) model [8, 9]. The evolution of the phase field is diffusive, and governed by a Swift-Hohenberg like free energy functional, which is minimized by a spatially-modulated equilibrium phase with the periodicity of the crystal lattice. The chosen free energy not only determines the crystal symmetry of the equilibrium phase, but all other thermodynamics quantities and response functions such as its elastic constants [8]. As it is generally the case with phenomenological free energies, it is only a function of a few free parameters, and hence the range of physical properties that can be attributed to the resulting macroscopic phase is somewhat limited. Nevertheless, the PFC model has been used in numerous numerical studies including crystal growth, grain boundaries and polycrystalline coarse graining phenomena [12, 27–30], strained epitaxial films [31], fracture propagation [8], plasticity avalanches from dislocation dynamics [32, 33], and edge dislocation dynamics [9]. It appears to us that this second approach is more natural from a physical point of view in that once the mesoscopic order parameter and the corresponding free energy are introduced, defect variables such as the Burgers vector and slip systems emerge as derived quantities. This seems preferable to introducing Ginzburg-Landau dynamics for slip system amplitudes defined a priori. Also, this second approach can nominally describe highly defected configurations in which a slip system, even in a coarse grained sense, can be difficult to define.

In this paper, we address the important theoretical question as to what extent the PFC model is actually capable of capturing mesoscopic plasticity mediated by dislocation dynamics. Although previous numerical simulations of dislocation dynamics [9, 33] suggest that dislocation motion is controlled by local stress, a theoretical derivation from the PFC model is still lacking. To address this question, we consider the PFC model and its amplitude expansion formulation, where we can show that the complex amplitudes are order parameters that support topological defects corresponding to dislocations in the crystal ordered phase. This allows us to accurately define a Burgers vector density field from the topological charges and predict the dislocation velocity directly from the dissipative relaxation of the amplitudes. We show that elastic stresses can be obtained from the PFC free energy functional through standard variational means, and recover known expressions for the linear elastic constants of the medium. Furthermore, we show that the dislocation velocity, near the bifurcation from the disordered state, follows the Peach-Koehler's force and is given by the product of Burgers vector and the elastic stress. Our theoretical predictions are consistent with previous numerical PFC studies of dislocation dynamics [9, 34].

The rest of the paper is organized as follows: In Section II, the phase field crystal model and its elastic equilibrium properties are discussed for the two dimensional case. Here, we also derive the elastic stress by variation of the free energy functional, and express it in terms of the crystal density field. Plastic motion mediated by dislocation dynamics is treated in Section III, where we use the amplitude expansion and the connection to an order parameter that supports topological defects. In Section IV, we verify the theoretical results by direct numerical simulations of the PFC model for a hexagonal lattice with a dislocation dipole. Summary and concluding remarks are presented in Section V.

II. LINEAR ELASTICITY IN THE PHASE FIELD CRYSTAL MODEL

The phase field crystal model that we employ involves a single scalar field $\psi(\mathbf{r}, t)$, function of space $\mathbf{r}$ in two-dimensions (2D) and time t, and a phenomenological free energy given by [9]

$$\begin{aligned} \mathcal{F}[\psi] &= \int d^2\mathbf{r}\; f\left(\psi, \nabla^2\psi\right) \\ &= \int d^2\mathbf{r} \left[\frac{1}{2}[(\nabla^2+1)\psi]^2 + \frac{r}{2}\psi^2 + \frac{1}{4}\psi^4\right], \end{aligned} \tag{3}$$

where r is a dimensionless parameter. In equilibrium, the free energy functional (3) is minimized with respect to ψ while keeping the average density constantly equal to ψ_0, so that $\left(\frac{\delta\mathcal{F}}{\delta\psi}\right)_0 = \mu_0$ where μ_0 is a constant Lagrange multiplier. When $r > 0$, $\psi = \psi_0$ is the only stable solution, whereas for $r < 0$, equilibrium periodic solutions of unit

wavenumber are possible for stripes and hexagonal patterns in 2D [8]. The crystalline phase with density distribution $n(\mathbf{r})$ is related to the phase field crystal through $\psi(\mathbf{r},t) = n(\mathbf{r},t)/n_0 - 1$, where $n(\mathbf{r},t) = \sum_i \langle \delta(\mathbf{r}-\mathbf{r}_i)\rangle$ is the statistical average number density of the equivalent crystal, and n_0 its spatially averaged density.

We focus below on the range of parameters for which a 2D hexagonal lattice is the equilibrium solution [8]

$$\psi = \psi_0 + \sum_{\mathbf{g}} A_{\mathbf{g}}^{(0)} e^{i\mathbf{g}\cdot\mathbf{r}}, \tag{4}$$

where the sum extends over all reciprocal lattice vectors $\mathbf{g}$ of a hexagonal lattice. We distinguish below three reciprocal lattice wave vectors $\mathbf{q}_n$, of unit length in the dimensionless units of Eq. (3), which are given in Cartesian coordinates by,

$$\mathbf{q}_1 = \mathbf{j},\ \mathbf{q}_2 = \frac{\sqrt{3}}{2}\mathbf{i} - \frac{1}{2}\mathbf{j},\ \mathbf{q}_3 = -\frac{\sqrt{3}}{2}\mathbf{i} - \frac{1}{2}\mathbf{j}, \tag{5}$$

which fixes the lattice constant $a = \frac{4\pi}{\sqrt{3}}$. These three vectors satisfy the resonance condition $\sum_{n=1}^{3} \mathbf{q}_n = 0$. The corresponding amplitudes $A_n^{(0)}$ are all constant and equal.

We first examine the change in free energy $\Delta\mathcal{F} = \mathcal{F}[\psi(\mathbf{r}')] - \mathcal{F}[\psi(\mathbf{r})]$ due to a small affine distortion $\mathbf{r}' = \mathbf{r} + \mathbf{u}(\mathbf{r})$. The free energy change $\Delta\mathcal{F}[\psi,\mathbf{u}]$ associated with such a distortion is given, after a transformation of variables from $\mathbf{r}'$ to $\mathbf{r}$, by

$$\Delta\mathcal{F} = \int d^2\mathbf{r} \left\{ (1+\nabla\cdot\mathbf{u}) f[\psi(\mathbf{r}'), \nabla'^2\psi(\mathbf{r}')] - f(\psi, \nabla^2\psi) \right\}, \tag{6}$$

where the transformed derivatives are given by

$$\begin{aligned} \partial_i' &= \partial_i - (\partial_i u_j)\partial_j + \mathcal{O}\left(|\nabla u|^2\right), \\ \partial_{ij}'\psi &= \partial_{ij}\psi - \partial_i\left[(\partial_j u_k)\partial_k\psi\right] - (\partial_i u_k)\partial_{kj}\psi + \mathcal{O}\left(|\nabla u|^2\right). \end{aligned} \tag{7}$$

After a Taylor expansion of Eq. (6) for small deformation gradients $\partial_i u_j$, we obtain

$$\Delta\mathcal{F} = \int d^2\mathbf{r} \left[-\frac{\partial f}{\partial(\partial_i\psi)}(\partial_i u_j)\partial_j\psi - \frac{\partial f}{\partial(\partial_{ij}\psi)} \left\{ \partial_i\left[(\partial_j u_k)\partial_k\psi\right] + (\partial_i u_k)\partial_{kj}\psi \right\} + (\nabla\cdot\mathbf{u}) f \right] + \mathcal{O}\left(|\nabla u|^2\right). \tag{8}$$

Because of the translational invariance of $\mathcal{F}$, the change $\Delta\mathcal{F}$ does not depend on the distortion, but only on its spatial gradients. Furthermore, the first term on the r.h.s. vanishes since f does not depend on the gradient of ψ. The second term on the r.h.s. can be transformed to a total divergence term and one proportional to the deformation gradient. Changing summation indices in order to factor the deformation gradient out, and using Stokes' theorem on the divergence term, we obtain that

$$\Delta\mathcal{F} = \int d^2\mathbf{r}\ \mathcal{E} + \int dS_i \frac{\partial f}{\partial(\partial_{ij}\psi)}(\partial_j u_k)\partial_k\psi, \tag{9}$$

where $d\mathbf{S}$ is the surface element vector on the boundary of the integration domain and

$$\mathcal{E} = \left[-\frac{\partial f}{\partial(\partial_{ik}\psi)}\partial_{jk}\psi + \left(\partial_k \frac{\partial f}{\partial(\partial_{ik}\psi)}\right)\partial_j\psi + \delta_{ij} f \right]\partial_i u_j \tag{10}$$

Equation (9) yields the elastic stress defined as the conjugate to the displacement gradient

$$\begin{aligned} \sigma_{ij} &= \frac{\partial\mathcal{E}}{\partial(\partial_i u_j)} \\ &= -\frac{\partial f}{\partial(\partial_{ik}\psi)}\partial_{jk}\psi + \left(\partial_k \frac{\partial f}{\partial(\partial_{ik}\psi)}\right)\partial_j\psi + f\delta_{ij}. \end{aligned} \tag{11}$$

Substituting Eq. (3), the corresponding stress is in our case

$$\sigma_{ij} = \left[\partial_i\mathcal{L}\psi\right]\partial_j\psi - \left[\mathcal{L}\psi\right]\partial_{ij}\psi + f\delta_{ij}, \tag{12}$$

with $\mathcal{L} = 1+\nabla^2$. Hence the elastic stress can be straightforwardly evaluated from the phase field ψ. Below we will show that this stress gives rise to the expected stress-strain relation in the linear elasticity regime, in agreement with earlier results for modulated phases [35, 36].

The stress gives rise to a body force density $F_j = \partial_i\sigma_{ij}$ given by

$$F_j \ = \ \mathcal{L}^2\psi\partial_j\psi - \mathcal{L}\psi\mathcal{L}(\partial_j\psi) + \partial_i f. \tag{13}$$

For an incompressible deformation, the Jacobi determinant is unity, the second term is the gradient of $-\frac{1}{2}(\mathcal{L}\psi)^2$, and can be included into a pressure term $\partial_j p$ as a gradient force. Thus, we can write the body force up to its gradient force contributions as

$$F_j = \mu\partial_j\psi, \tag{14}$$

as the additional terms in the chemical potential $\mu = \frac{\delta\mathcal{F}}{\delta\psi} = \mathcal{L}^2\psi + r\psi + \psi^3$ also lead to gradient terms.

More generally, the additional contribution of a compressible deformation to the body force

$$\partial_i\left(\delta_{ij} f\right) = \partial_j f = \mathcal{L}\psi\mathcal{L}(\partial_j\psi) + r\psi\partial_j\psi + \psi^3\partial_j\psi. \tag{15}$$

Hence, the body force density induced by a deformation is the same in both the compressible and incompressible

cases (up to a gradient force in the incompressible case), and given as

$$F_j = \partial_i \sigma_{ij} = \left(\mathcal{L}^2\psi + r\psi + \psi^3\right)\partial_j\psi = \mu\partial_j\psi. \quad (16)$$

Thus, the body force associated with a small distortion in the phase field crystal density is expressed in general as $\mu\nabla\psi$. Analogous results have been derived by using microforce balances in the context of continuum mechanics [23], or invoking thermodynamic relations arising from broken symmetries [37].

In the weakly nonlinear region of $|r| \ll 1$, the order parameter ψ can be expanded in terms of the slowly varying amplitudes A_n of the resonant modes $\mathbf{q}_n$ of Eq. (5). A weakly distorted configuration relative to the reference hexagonal configuration can then be written in this expansion as [34, 38]

$$\psi = \psi_0 + \sum_n A_n e^{i\mathbf{q}_n\cdot(\mathbf{r}-\mathbf{u})} + c.c., \quad (17)$$

with both the mean density ψ_0 and the amplitudes A_n are slowly varying on length scales much larger than the lattice spacing. After straightforward differentiation of ψ in Eq. (17), we obtain that

$$\begin{aligned} \partial_i\left(\mathcal{L}\psi\right) &= 2iA_0\partial_l u_k \sum_{\mathbf{q}} q_l q_k q_i \exp\left[i\mathbf{q}\cdot(\mathbf{r}-\mathbf{u})\right], \\ \left[\partial_i\left(\mathcal{L}\psi\right)\right]\partial_j\psi &= -2A_0^2\partial_l u_k \sum_{\mathbf{q},\mathbf{q}'} q_l q_k q_i q'_j \\ &\quad \times \exp\left[i(\mathbf{q}+\mathbf{q}')\cdot(\mathbf{r}-\mathbf{u})\right], \end{aligned} \quad (18)$$

where the sums involve the components of the vectors $\pm\mathbf{q}_n$, the negative vectors included for the complex conjugate (we have dropped the subindex n for ease of notation). Similarly, we find

$$[\mathcal{L}\psi]\partial_{ij}\psi = -\psi_0 A_0 \sum_{\mathbf{q}} \left(q_i q_j - q_i q_k \partial_j u_k - q_j q_k \partial_i u_k\right)\exp\left[i\mathbf{q}\cdot(\mathbf{r}-\mathbf{u})\right] - 2A_0^2\partial_l u_k \sum_{\mathbf{q},\mathbf{q}'} q_l q_k q'_i q'_j \exp\left[i(\mathbf{q}+\mathbf{q}')\cdot(\mathbf{r}-\mathbf{u})\right]. \quad (19)$$

Finally, by averaging this result over a unit cell of the lattice, and given that the slowly varying deformation gradients are constant over a lattice spacing, all single $\mathbf{q}$ terms vanish, whereas $\exp[i(\mathbf{q}+\mathbf{q}')\cdot(\mathbf{x}-\mathbf{u})]$ factors integrate to $\delta_{\mathbf{q},-\mathbf{q}'}$. Therefore the averaged stress field from Eq. (12) becomes

$$\langle\sigma_{ij}\rangle = 4A_0^2\partial_l u_k \sum_{\mathbf{q}} q_l q_k q_i q_j. \quad (20)$$

Since the coefficients multiplying $\partial_l u_k$ are symmetric under the interchange $l \leftrightarrow k$, we can also write the relation in terms of the symmetrized strain $u_{lk} = \frac{1}{2}(\partial_l u_k + \partial_k u_l)$. Reintroducing the vectors $\mathbf{q}_n$ and their negatives $-\mathbf{q}_n$ explicitly, we find

$$\langle\sigma_{ij}\rangle = 8A_0^2 u_{lk} \sum_{n=1}^{3} q_i^n q_j^n q_k^n q_l^n. \quad (21)$$

Equation (21) is a linear stress-strain relationship which only depends on three crystal reciprocal lattice vectors and the slowly varying amplitudes. For a hexagonal lattice, inserting the reciprocal lattice vectors given in Eq. (5) yields $C_{11} = C_{22} = 9A_0^2$, $C_{12} = 3A_0^2$ and $C_{44} = 3A_0^2$ (cf., e.g., Ref. [9]). This result can also be written in terms of Lamé coefficients as $\langle\sigma_{ij}\rangle = \lambda\delta_{ij}u_{kk} + 2\mu u_{ij}$ with $\lambda = \mu = 3A_0^2$, giving a Poisson's ratio of $\nu = \frac{\lambda}{2(\lambda+\mu)} = \frac{1}{4}$. This is different from the Poisson's ratio of $\frac{1}{3}$ obtained in Ref. [28], as they use the plane stress condition, while we are assuming plane strain without loss of generality.

III. PLASTIC FLOW AND DISLOCATION DYNAMICS

At the mesoscale level, the evolution of the phase field is driven by local relaxation of the free energy functional,

$$\frac{\partial\psi}{\partial t} = \nabla^2\frac{\delta\mathcal{F}}{\delta\psi}, \quad (22)$$

where we have assumed a constant mobility coefficient (equal to unity in rescaled units). Equation (22) governs both conservation of mass and the evolution of crystal deformations. We will focus here on 2D systems, although a similar development can be applied in three dimensions.

There are no topological singularities in the phase field $\psi(\mathbf{r}, t)$. However, under conditions in which the amplitude expansion of Eq. (4) is valid (mean density ψ_0 and amplitudes A_n that vary on length scales much larger than the wavelength of the reference pattern), topological defects can be identified from the location of the zeros of the complex amplitudes [39, 40]. Evolution equations for ψ_0 and A_n have been derived by several techniques, such as Renormalization Group methods [41] and multiple-scale analysis [42]. In the lowest derivative approximation that preserves the rotational invariance of the phase

field model [43], the resulting equations are given as [42]

$$\begin{aligned}\frac{\partial\psi_0}{\partial t} &= \nabla^2\Big[(1+\nabla^2)^2\psi_0+\psi_0^3+6\psi_0\textstyle\sum_n|A_n|^2 \\ &\qquad +6\left(\textstyle\prod_n A_n+c.c.\right)\Big], \\ \frac{\partial A_n}{\partial t} &= -\mathcal{L}_n^2A_n-(3\psi_0^2+r)A_n-6\psi_0\textstyle\prod_{m\neq n}A_m^* \\ &\qquad -3A_n\left(2\textstyle\sum_m|A_m|^2-|A_n|^2\right),\end{aligned} \tag{23}$$

where $n=1,2,3$, $\mathcal{L}_n=\nabla^2+2i\mathbf{q}_n\cdot\nabla$ and $\mathbf{q}_n$ are the three reciprocal vectors of Eq. (5). Variation of ψ_0 at constant A_n needs to be interpreted as vacancy diffusion. These amplitude equations are themselves variational, and can be written as [42],

$$\begin{aligned}\frac{\partial\psi_0}{\partial t} &= \nabla^2\frac{\delta\mathcal{F}_{CG}}{\delta\psi_0} \\ \frac{\partial A_n}{\partial t} &= -\frac{\delta\mathcal{F}_{CG}}{\delta A_n^*}.\end{aligned} \tag{24}$$

where $\mathcal{F}_{CG}\{\psi_0,A_n\}$ is the free energy, function of the amplitudes alone. Recall that all of these equations ignore higher Fourier components $|\mathbf{q}|>1$, so they are only valid close to the bifurcation point, $|r|\ll 1$.

A. Transformation of field singularities to dislocation coordinates

In order to make contact with the classical macroscopic description of plastic motion in terms of the velocity of a dislocation element under an imposed stress, we describe the transformation of variables that is required to relate the evolution of the phase field to the motion of the singularities associated with the amplitudes. Assume a spatial distribution of point dislocations and define a Burger's vector density as $\mathbf{B}(\mathbf{r})=\sum_\alpha\mathbf{b}_\alpha\delta(\mathbf{r}-\mathbf{r}_\alpha)$, where $\mathbf{r}_\alpha$ is the location of the dislocation with Burger's vector $\mathbf{b}_\alpha$ in some element of volume. For each Burger's vector $\mathbf{b}_\alpha$ we define the three integers $s_n^\alpha=\frac{1}{2\pi}(\mathbf{q}_n\cdot\mathbf{b}_\alpha)$, which satisfy the relation $\sum_{n=1}^3 s_n^\alpha=\frac{1}{2\pi}\mathbf{b}_\alpha\cdot\sum_{n=1}^3\mathbf{q}_n=0$.

A dislocation at $\mathbf{r}_\alpha$ corresponds to a discontinuous deformation field $\mathbf{u}(\mathbf{r})$ with $\oint d\mathbf{u}=\mathbf{b}_\alpha$ around a contour containing only $\mathbf{r}_\alpha$. This deformation field is associated with a phase factor in the complex amplitudes, given by $A_n(\mathbf{r})=|A_n|e^{-i\mathbf{q}_n\cdot\mathbf{u}+i\phi}$, with $\phi(\mathbf{r})$ smooth inside the contour. The phase circulation of the amplitude around the same contour can then be found as

$$\begin{aligned}\oint d(\arg A_n) &= -q_j^n\oint\partial_k u_j dr_k+\oint\partial_k\phi dr_k \\ &= -q_j^nb_j^\alpha=-2\pi s_n^\alpha,\end{aligned} \tag{25}$$

using that ϕ has no circulation, being smooth inside the contour. Thus the amplitude A_n has a vortex with winding number $-s_n^\alpha$ at $\mathbf{r}=\mathbf{r}_\alpha$. This induces the following transformation of delta functions [44–47]

$$\begin{aligned}D_n\delta(A_n) &= -\sum_\alpha s_n^\alpha\delta(\mathbf{r}-\mathbf{r}_\alpha) \\ &= -\frac{1}{2\pi}\sum_\alpha(\mathbf{q}_n\cdot\mathbf{b}_\alpha)\delta(\mathbf{r}-\mathbf{r}_\alpha),\end{aligned} \tag{26}$$

for a given amplitude A_n, where

$$D_n=\mathrm{Im}\left(\partial_xA_n^*\partial_yA_n\right)=\frac{1}{2i}\epsilon_{ij}\partial_iA_n^*\partial_jA_n, \tag{27}$$

is the Jacobian of the transformation from complex amplitudes A_n to vortex coordinates $\mathbf{r}_\alpha$, and ϵ_{ij} is the antisymmetric tensor. Multiplying the above expression with a reciprocal vector $\mathbf{q}_n$ and summing over n, we find the dislocation density as

$$\mathbf{B}(\mathbf{r})=-\frac{4\pi}{3}\sum_{n=1}^3\mathbf{q}_nD_n\delta(A_n), \tag{28}$$

by making use of the fact that $\sum_{n=1}^3 q_i^nq_j^n=\frac{3}{2}\delta_{ij}$ (see appendix A for why we use reciprocal lattice vectors in this expansion rather than real space lattice vectors).

In order to obtain the equation governing the motion of the Burgers vector density, we use that the determinant fields D_n have conserved currents given by [47]

$$J_k^{(n)}=\frac{1}{2i}\epsilon_{kl}\left(\frac{\partial A_n}{\partial t}\partial_lA_n^*-\frac{\partial A_n^*}{\partial t}\partial_lA_n\right)=\epsilon_{kl}\,\mathrm{Im}\left(\frac{\partial A_n}{\partial t}\partial_lA_n^*\right), \tag{29}$$

so that $\frac{\partial D_n}{\partial t}=-\partial_kJ_k^{(n)}$, as can be verified by substitution. The amplitude evolution at the vortex location $\frac{\partial A_n}{\partial t}$ can be found from an amplitude expansion of $\frac{\partial\psi}{\partial t}$, such as Eq. (23).

We also have a similar continuity equation for the delta functions,

$$D_n\frac{\partial}{\partial t}\delta(A_n)=-J_i^{(n)}\partial_i\delta(A_n), \tag{30}$$

which can be proved by differentiating through the delta functions and inserting for D_n and $J_i^{(n)}$. Hence, differentiating the dislocation density with time, we find the Burger's vector current

$$\begin{aligned}\frac{\partial B_i}{\partial t} &= -\frac{4\pi}{3}\sum_{n=1}^3 q_i^n\left(\frac{\partial D_n}{\partial t}\delta(A_n)+D_n\frac{\partial}{\partial t}\delta(A_n)\right) \\ &= \frac{4\pi}{3}\sum_{n=1}^3 q_i^n\left(\partial_jJ_j^{(n)}\delta(A_n)+J_j^{(n)}\partial_j\delta(A_n)\right) \\ &= \partial_j\left(\frac{4\pi}{3}\sum_{n=1}^3 q_i^nJ_j^{(n)}\delta(A_n)\right)=-\partial_j\mathcal{J}_{ij}.\end{aligned} \tag{31}$$

Whenever $D_n=0$ we have $\delta(A_n)=0$, otherwise we can

transform back to physical coordinates using Eq. (26),

$$\begin{aligned}\mathcal{J}_{ij} &= -\frac{4\pi}{3}\sum_{n=1}^{3} q_i^n J_j^{(n)}\delta(A_n) \\ &= \frac{2}{3}\sum_{n=1}^{3} q_i^n J_j^{(n)} \sum_\alpha \frac{\mathbf{q}_n\cdot\mathbf{b}_\alpha}{D_n}\delta(\mathbf{r}-\mathbf{r}_\alpha). \end{aligned} \tag{32}$$

On the other hand, if the dislocations are moving with velocity $\mathbf{v}_\alpha$, we have

$$\mathcal{J}_{ij} = \sum_\alpha b_i^\alpha v_j^\alpha \delta(\mathbf{r}-\mathbf{r}_\alpha). \tag{33}$$

Hence, equating the two expressions for $\mathcal{J}_{ij}$ at $\mathbf{r}=\mathbf{r}_\alpha$ and contracting with the burger's vector $\mathbf{b}_\alpha$, we find

$$v_j^\alpha = \frac{2}{3}\sum_{n=1}^{3}\frac{(\mathbf{q}_n\cdot\mathbf{b}_\alpha)^2}{|\mathbf{b}_\alpha|^2}\frac{J_j^{(n)}}{D_n} = \frac{1}{S_\alpha^2}\sum_{n=1}^{3}(s_n^\alpha)^2\frac{J_j^{(n)}}{D_n}, \tag{34}$$

where we set $S_\alpha^2 = \sum_{n=1}^3 (s_n^\alpha)^2$ and used that $|\mathbf{b}_\alpha|^2 = \frac{8}{3}\pi^2 S_\alpha^2$. This is a general result and the central relation between the velocity of a point singularity and the equation governing the evolution of the phase field amplitudes. We apply this expression below to obtain an estimate of the velocity response of a single point dislocation under an applied strain.

B. Dislocation motion

At a dislocation core, assumed at $\mathbf{r}=0$, the amplitude A_n will vanish as long as $2\pi s_n = \mathbf{q}_n\cdot\mathbf{b} \neq 0$. Since $s_1+s_2+s_3=0$, any dislocation must give rise to vortices in at least two of the three amplitudes, and so these two amplitudes vanish. This means that the amplitude evolution equation (23) for vanishing amplitudes at the dislocation position reduces to

$$\frac{\partial A_n(\mathbf{r}=0)}{\partial t} \approx -\mathcal{L}_n^2 A_n\Big|_{\mathbf{r}=0} \tag{35}$$

whenever $s_n \neq 0$. The equations governing the defect amplitudes entering Eq. (34) decouple, and hence we can study the motion of each amplitude independently.

We now consider a dislocation which would be stationary in the absence of any externally imposed stress, $\mathcal{L}_n^2 A_n\Big|_{\mathbf{r}=0} = 0$. If a smooth deformation $\tilde{\mathbf{u}}$, is imposed in addition to the singular deformation field associated with the stationary dislocation, the total displacement field can be written as $\mathbf{u} = \mathbf{u}^{\text{sing}} + \tilde{\mathbf{u}}$. This displacement includes the singular deformation $\mathbf{u}^{\text{sing}}$ for the stationary dislocation described by the amplitudes A_n, and a smooth "phonon" part (e.g., as described in ref. [25, Eq. (2.8a)]). The defect amplitude under this distortion is $\tilde{A}_n = A_n e^{-i\mathbf{q}_n\cdot\tilde{\mathbf{u}}+h_n(\mathbf{r})}$, where the unknown function h_n models how the defect core responds to the deformation [46]. We assume that these core perturbations are small compared to the driving force due to the deformation gradient, $|\nabla h_n| \ll |\nabla\tilde{\mathbf{u}}|$, and neglect them. The applied smooth deformation will cause the dislocation to move,

$$\partial_t \tilde{A}_n = -\mathcal{L}_n^2\tilde{A}_n \neq 0, \tag{36}$$

and our aim is to compute how the resulting dislocation motion depends on the imposed deformation.

Let us focus on one particular n and write $\tilde{A} = Ae^{-i\mathbf{q}\cdot\tilde{\mathbf{u}}}$, with its associated wave vector $\mathbf{q}$. Then,

$$\begin{aligned}\partial_i\tilde{A} &= (\partial_i A - iAq_k\partial_i\tilde{u}_k)\, e^{-i\mathbf{q}\cdot\tilde{\mathbf{u}}} \\ \partial_{ij}\tilde{A} &= (\partial_{ij}A - i\partial_i A q_k\partial_j\tilde{u}_k - i\partial_j A q_k\partial_i\tilde{u}_k)\, e^{-i\mathbf{q}\cdot\tilde{\mathbf{u}}}. \end{aligned} \tag{37}$$

Continuing in this manner and using that A is the stationary vortex solution ($\mathcal{L}^2 A = 0$), we then have that

$$\partial_t\tilde{A} \;=\; -\mathcal{L}^2\tilde{A} = 4iq_j[(\partial_i + iq_i)\mathcal{L}A]\partial_i\tilde{u}_j e^{-i\mathbf{q}\cdot\tilde{\mathbf{u}}}. \tag{38}$$

If $s=\pm1$, one solution of $\mathcal{L}^2 A = 0$ is the isotropic vortex solution $A \propto x - isy$. We will assume the vortex takes this form, although other solutions are possible. For this solution, we have $\mathcal{L}A = 2iq_k\partial_k A$ and $\partial_i\mathcal{L}A = 0$. Hence $\partial_t\tilde{A}$ simplifies to

$$\partial_t\tilde{A} = -8iq_iq_jq_k\partial_k A\partial_i\tilde{u}_j e^{-i\mathbf{q}\cdot\tilde{\mathbf{u}}}. \tag{39}$$

Inserting this into to the defect current in Eq. (29), we find

$$J_i \;=\; -8\epsilon_{ij}q_kq_lq_m\partial_k\tilde{u}_l\,\mathrm{Im}\left(i\partial_m A\partial_j A^*\right). \tag{40}$$

Since the defect density is unchanged under the smooth deformation, the Jacobi determinant at the dislocation position is unchanged,

$$D = \frac{1}{2i}\epsilon_{ij}\partial_i\tilde{A}^*\partial_j\tilde{A} = \frac{1}{2i}\epsilon_{ij}\partial_i A^*\partial_j A. \tag{41}$$

The isotropic vortex $A\propto x-isy$ satisfies

$$i\partial_i A = -\frac{1}{s}\epsilon_{ij}\partial_j A, \tag{42}$$

so that

$$J_i = \frac{8}{s}\epsilon_{ij}\epsilon_{mo}q_kq_lq_m\partial_k\tilde{u}_l\,\mathrm{Im}\left(\partial_o A\partial_j A^*\right). \tag{43}$$

We can show that $\mathrm{Im}(\partial_o A\partial_j A^*) = \epsilon_{jo}D$, which means that

$$J_i = \frac{8}{s}\epsilon_{ij}q_jq_kq_l\partial_k\tilde{u}_l D. \tag{44}$$

Thus, for a simple dislocation with all $|s_n|\leq 1$, we find that the vortex velocity from Eq. (34) is

$$\begin{aligned} v_i \;&=\; \frac{8\epsilon_{ij}}{S^2}\sum_{n=1}^{3} s_n q_j^n q_k^n q_l^n\partial_k\tilde{u}_l \\ &=\; \frac{4b_m}{\pi S^2}\epsilon_{ij}\sum_{n=1}^{3} q_m^n q_j^n q_k^n q_l^n\partial_k\tilde{u}_l \\ &=\; \frac{1}{4\pi A_0^2}\epsilon_{ij}\left\langle\tilde{\sigma}_{jk}\right\rangle b_k, \end{aligned} \tag{45}$$

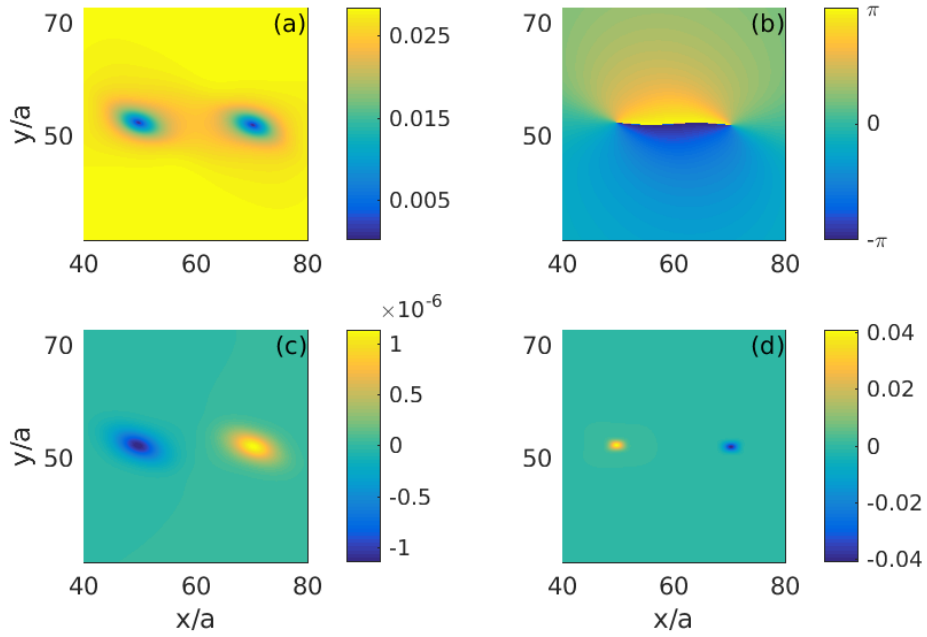

FIG. 1: (a) and (b): Magnitude and phase of the A_2 amplitude, showing the initial vortices corresponding to the initial dislocations. (c): The D_2 field showing the sign of the vortex charge. (d): The resulting B_x dislocation density in the x direction, with $w = A_0/5$. x and y is given in units of the lattice constant $a = \frac{4\pi}{\sqrt{3}q_0}$.

where we used the stress-strain relation from Eq. (21) to relate the gradient of the smooth deformation $\tilde{\mathbf{u}}$ to its associated stress $\tilde{\sigma}_{ij}$.

Thus, we obtain an expression for the dislocation velocity which agrees with the Peach-Koehler force of classical dislocation theory [4], and gives an explicit form of the dislocation mobility. The derivation has excluded the singular deformation $\mathbf{u}^{\text{sing}}$ associated with the dislocation, as well as any defect core variations in the amplitudes which would be contained in the functions $h_n(\mathbf{r})$. Within our approximations, the mobility coefficient is isotropic. This probably follows from our assumption that the vortex solution of $\mathcal{L}_n^2 A_n = 0$ is isotropic.

In what follows, we calculate numerically the dislocation velocity by tracking the position of the dislocation and compare it with the velocity determined by Eq. (34) from the topological defect currents. We also discuss the numerical challenge to verify the overdamped motion with isotropic mobility and following the Peach-Koehler force according to Eq. (45), as well as the extent to which we expect this to be valid.

IV. NUMERICAL RESULTS

We test our predictions by directly simulating a perfect hexagonal crystal containing a dislocation dipole in two scenarios of pure glide and pure climb, respectively. The dislocations move under the mutual interaction force between them until they annihilate.

We use two parameter sets $r = -0.01$ and $\psi_0 = -0.04$ (small amplitude near the bifurcation) and $r = -0.8$ and $\psi_0 = -0.43$ (finite amplitude). The initial state is prepared by setting $\psi(\mathbf{r}) = \psi_0 + \sum_n A_n e^{i\mathbf{q}_n\cdot\mathbf{r}} + c.c.$, where the amplitudes contain vortices with the appropriate charges for each dislocation $A_n = A_0 \exp\left[-\sum_\alpha i s_n^\alpha \theta(\mathbf{r} - \mathbf{r}_\alpha)\right]$. We use two different initial geometries for measuring glide and climb motion. For the glide case, we put two dislocations with opposite Burger's vectors pointing along the x direction, i.e $\mathbf{b} = (\pm a, 0)$, and located in the same glide plane on the x axis with some initial separation. For climb, we place the same dislocations directly above each other on the y axis, on different glide planes. We then evolve Eq. (22) using an exponential time differencing method [48], and track the motion of dislocations as topological defects.

The amplitudes of the phase field are computed by performing a local amplitude decomposition, which corresponds to averaging $\psi e^{-i\mathbf{q}\cdot\mathbf{r}}$ over a region roughly corresponding to a lattice unit cell [49]. For numerical stability we use a convolution with a Gaussian of width $a = 2\pi/\sqrt{3}$ instead of hard limits to the averaging region. This convolution is most efficiently evaluated in Fourier space, using the expression

$$A_n(\mathbf{r}) = e^{-i\mathbf{q_n}\cdot\mathbf{r}} F^{-1}\left\{ e^{-\frac{8}{3}\pi^2(\mathbf{k}-\mathbf{q}_n)^2} F[\psi] \right\}, \qquad (46)$$

where F and F^{-1} denote the Fourier and inverse Fourier transforms, respectively. Similarly, the time evolution of the amplitude can be extracted from the PFC dynamics

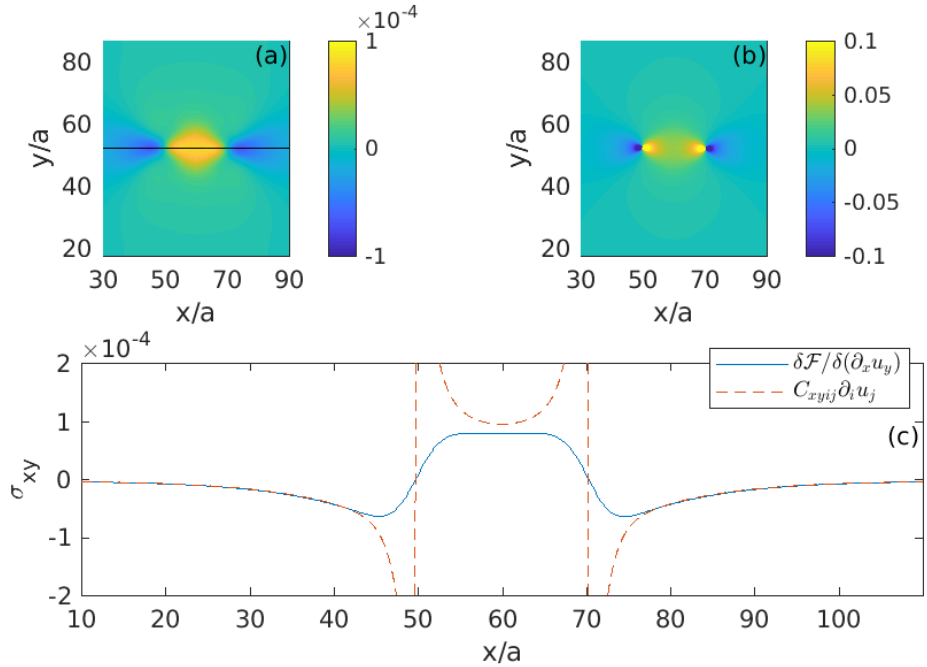

FIG. 2: (a): Map of the stress field $\langle\sigma_{xy}\rangle$, as computed directly from the formula in eq. (12), with a Gaussian average. (b): Map of the strain field $\partial_y u_x$, computed from the amplitudes by eq. (50). Note that the color scale is saturated, and the measured strain field diverges at the dislocation. (c): Comparison of the stress computed along the indicated horizontal line in two different ways: Using the direct expression for the stress in Eq. (12) (solid line), and using the stress-strain relation from Eq. (21) (dashed line). Both expressions agree in the crystal bulk, but break down close to the dislocation.

as

$$\frac{\partial A_n(\mathbf{r})}{\partial t} = e^{-i\mathbf{q_n}\cdot\mathbf{r}} F^{-1}\left\{ e^{-\frac{8}{3}\pi^2(\mathbf{k}-\mathbf{q}_n)^2} F\left[\frac{\partial\psi}{\partial t}\right]\right\}, \quad (47)$$

Figure 1 shows the magnitude and phase of the complex amplitude A_2 for the initial dislocation dipole after a short period of relaxation (panels a-b). From the amplitudes we can calculate a Gaussian approximation to the $\delta(A_n)$ function as

$$\delta(A_n) = \frac{1}{2\pi w^2} e^{-\frac{|A_n|^2}{2w^2}}, \quad (48)$$

where smaller w's give sharper delta functions. Along with the D_n fields obtained by numerically differentiating the amplitudes (Fig. 1, panel c), we obtain approximations to the Burger's vector density from Eq. (28), shown in Fig. 1, panel (d).

The total displacement field away from defect cores can be obtained by writing $A_n = |A_n| e^{-i\mathbf{q}_n\cdot\mathbf{u}}$, so that

$$\mathrm{Im}\,\frac{\partial_j A_n}{A_n} = -q_k^n \partial_j u_k. \quad (49)$$

This relation can be inverted to find

$$\partial_j u_k = -\frac{2}{3}\sum_n q_k^n\,\mathrm{Im}\,\frac{\partial_j A_n}{A_n}, \quad (50)$$

thus giving numerical values for the total strain. Figure 2 summarizes our results. We show the distortion $\partial_x u_y$ given by Eq. (50) along with the corresponding stress field evaluated from Eq. (12) with a Gaussian average. Of course, this stress-strain relation is not expected to hold near the defect cores where the distortion is large. However, we also plot the shear stress as a function of y along the line shown in the figure, and show that the linear stress-strain relation, Eq. (21), does hold away from the cores.

Properties of a given dislocation can be computed by taking averages weighted by the Burger's vector density $\mathbf{B}(\mathbf{r})$ inside a thresholded region. Thus we compute the location of each dislocation by taking centers of mass of the Burger's vector density, and dislocation speeds by averaging the topological defect currents of Eq. (34). In Figure 3, we compare glide and climb velocities predicted from Eq. (34), and a direct numerical determination of the velocities by performing a finite time difference between successive dislocation positions. In panels (a) and (b), the glide and climb velocities are presented for small $|r|$, showing excellent agreement. The glide velocity for finite r is presented in panel (c), and shows a stick and slip like behavior with periodicity related to the lattice constant a, consistent with previous numerical simulations from Ref. [9]. These are lattice effects affecting the motion of the amplitudes when r is not small due to nonlinear couplings, the phase field analog of Peierls pinning stresses [50]. Note that we observe no climb motion at the deep quench parameter $r = -0.8$.

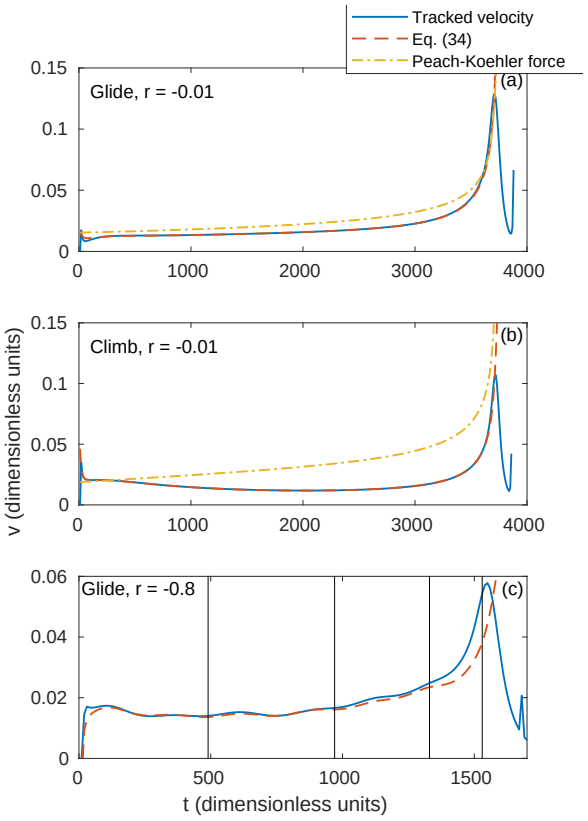

FIG. 3: The dislocation velocity as a function of time until the annihilation time for low quenches (panels a and b) versus deep quenches (panel c), given in the dimensionless units of Eq. (22). In panel (c), vertical lines indicate points in time where the dislocation has traveled a distance a from its initial point.

The velocity computations shown are robust with respect to the delta function width parameter w from Eq. (48). However, the dislocation center of mass location used in the tracked velocity shows artificial fluctuations for width parameters larger than $\approx A_0/20$.

Directly verifying the Eq. (45) is more difficult due to the required separation of stress fields into a singular part and a phonon part $\tilde{\sigma}_{ij}$. Furthermore, $\tilde{\sigma}_{ij}$ needs to be in mechanical equilibrium during the PFC evolution. As an indirect test, one can assume as a first approximation that the stress field on each dislocation is due only to the other, and it is approximately given by the shear stress induced by an edge dislocation in an infinite space

$$\sigma_{xy} = \frac{b}{2\pi}\frac{2\mu(\lambda+\mu)}{\lambda+2\mu}\frac{\cos\phi\cos 2\phi}{d},$$
$$\sigma_{xx} = -\frac{b}{2\pi}\frac{2\mu(\lambda+\mu)}{\lambda+2\mu}\frac{\sin\phi(2+\cos 2\phi)}{d}, \qquad (51)$$

where d and ϕ are the instantaneous distance and angle between the dislocations, respectively. Inserting this expression into Eq. (45) and using appropriate values for the angle ϕ for the glide and climb geometries, we find

$$v_x^{\rm glide} = v_y^{\rm climb} = \pm\frac{a^2}{2\pi^2 d}, \qquad (52)$$

with the sign depending on which of the two dislocations we are considering. This equilibrium velocity is denoted as "Peach-Koehler force" in Fig. 3 (panels a,b). For glide velocity we find a reasonable agreement with the measured velocity, but the climb velocity shows a different functional form. The deviations from the predicted evolution from Eq. (52) are due to simplifying assumptions used in deriving the Peach-Koehler force, the most important being the isotropic solution of the stationary vortex structure. In practice, the profile of the vortex near the core maybe anisotropic and dependent on the driving force. This means that the core structure would deform in the presence of external forces, which would be described by having the $h_n(\mathbf{r})$ functions depend on $\tilde{\mathbf{u}}$. Note that the decoupling of the amplitude equations and the assumption of an isotropic vortex solution were what allowed us to ignore the effect of vacancies. It is known that vacancy diffusion is important for climb motion, and therefore we expect greater deviations from the theoretical prediction in the case of climb, as it is also evidenced in Fig. 3 panel (c).

V. CONCLUSIONS AND DISCUSSION

We have introduced a phase field model of a crystalline phase to describe the topological singularity that corresponds to isolated dislocations. The phase field itself is regular (non singular) at defect cores. The singularity appears through consideration of the slowly varying amplitudes or envelopes of the phase field in a macroscopically defected configuration. These amplitudes allow the computation of local stresses near the defect, as well as the velocity of the point defect from the kinetic equations governing the evolution of the phase field. The combination of both results allows the derivation of the classical Peach-Koehler force on the defect as well as an explicit calculation of the defect mobility, although these depend sensitively on the dislocation core structure. Our main results have been verified by direct numerical solution of the equation governing the evolution of the phase field for the case of a dislocation dipole in a two dimensional hexagonal lattice.

Phase field crystal models of the type discussed in this paper lack a dependence on lattice deformation as an independent variable. However, we have shown explicitly that it is possible to calculate the *elastic* stress directly from the phase field free energy by considering its variation with respect to a suitably chosen phase field distortion. The stress thus derived is consistent with linear elasticity and leads to known expressions for the elastic constants of the phase field crystal. Furthermore, the phase field description can also describe defected configurations. While the phase field remains nonsingular no

matter how large the local distortion of the reference configuration is, the location of any isolated singularities can be accomplished through the determination of the zeros of a slowly varying (on the scale of the periodicity of the field) complex amplitude or envelope of the phase field. Such a coarse graining is essential to defining singular fields from the regular phase field. On this slow scale, we have then derived the Peach-Koehler force on a topological defect, subject to some simplifying assumptions. As expected, this force depends only on a slowly varying stress (distortion), and not on other fast variations of the phase field near the defect that constitute the singular strain field. However, more work is needed to fully understand the effect of the core structure and vacancy diffusion on this Peach-Kohler force.

Our results also clarify the relationship between dissipative relaxation of the phase field and plastic motion. Equation (45) relates the velocity of a dislocation with its Burgers vector and the *slowly* varying stress $\langle\tilde{\sigma}_{ij}\rangle$. Such a relation follows directly from the equation governing the relaxation of the phase field, Eq. (22), in the range of $r \ll 1$ in which it can be described by an amplitude equation. This equation also gives an explicit expression for the dislocation mobility which depends on the specific functional form of the free energy considered. More generally, the role of the free energy functional introduced includes the definition of a Burgers vector scale, and topological charge conservation over large length scales. Of course, any fast variations of the phase field near defects are still described and very much included in Eq. (22). Short scale effects such as dislocation creation and annihilation, and any nonlinearities of both elastic and plastic origin evolve according to the dissipative evolution of the phase field.

Acknowledgments

This research has been supported by a startup grant from the University of Oslo, and by the National Science Foundation under contract DMS 1435372

Appendix A: Calculation of the dislocation current

Equation (28) gives an expression for the dislocation density in terms of the three reciprocal lattice vectors $\mathbf{q}_n$. Since the Burger's vector is a vector in the real space lattice, it would seem more natural to express the dislocation density in terms of the two real space lattice vectors $\mathbf{a}_n$, where $\mathbf{q}_n \cdot \mathbf{a}_m = 2\pi\delta_{mn}$ (for $n, m = 1, 2$). Indeed, using that $\sum_{n=1}^{2} a_i^n q_j^n = 2\pi\delta_{ij}$, we find the alternative expression

$$\mathbf{B}(\mathbf{r}) = -\sum_{n=1}^{2} \mathbf{a}_n D_n \delta(A_n), \tag{A1}$$

which of course is equal to Eq. (28). Going through the same derivation as in section III A leads to a Burger's vector current

$$\mathcal{J}_{ij} = -\sum_{n=1}^{2} a_i^n J_j^{(n)} \delta(A_n), \tag{A2}$$

however this current does not agree with the current in Eq. (32).

The missing point is that the conservation equation for the field $D_n\delta(A_n)$,

$$\partial_t [D_n \delta(A_n)] + \partial_i [J_i^{(n)} \delta(A_n)] = 0, \tag{A3}$$

only determines its current $I_j^{(n)}$ up to an unknown divergence-free vector field $K_j^{(n)}$, i.e.

$$I_i^{(n)} = J_i^{(n)} \delta(A_n) + K_i^{(n)}, \tag{A4}$$

where $\partial_i K_i^{(n)} = 0$. To determine this residual current, we observe that

$$\sum_{n=1}^{3} D_n \delta(A_n) = -\frac{1}{2\pi} \sum_{\alpha} b_i^{\alpha} \delta(\mathbf{r} - \mathbf{r}_\alpha) \sum_{n=1}^{3} q_i^n = 0, \tag{A5}$$

due to the resonance condition $\sum_n \mathbf{q}_n = 0$. Hence it is natural to require that the current of this field vanishes identically,

$$\sum_{n=1}^{3} I_i^{(n)} = \sum_{n=1}^{3} J_i^{(n)} \delta(A_n) + \sum_{n=1}^{3} K_i^{(n)} = 0. \tag{A6}$$

This condition is fulfilled by setting $K_i^{(n)} = -\frac{1}{3}\sum_{m=1}^{3} J_i^{(m)} \delta(A_m)$, which has vanishing divergence. With this choice, the dislocation current in Eq. (32) is modified to

$$\mathcal{J}_{ij} = -\frac{4\pi}{3} \sum_{n=1}^{3} q_i^n J_j^{(n)} \delta(A_n) + \frac{4\pi}{9} \sum_{n=1}^{3} q_i^n \sum_{m=1}^{3} J_j^{(m)} \delta(A_m), \tag{A7}$$

where the second term vanishes due to resonance. Hence the additional fields $K_i^{(n)}$ give no contribution when we express $\mathbf{B}(\mathbf{r})$ in terms of the three reciprocal lattice vectors. On the other hand, if we used real lattice vectors $\mathbf{a}_n$ instead, the extra term would not vanish.

[1] J. Weiss and D. Marsan, Science **299**, 89 (2003).
[2] M. Zaiser and P. Moretti, J. Stat. Mech.: Theory and Experiment **2005**, P08004 (2005).
[3] J. Weiss, W. B. Rhouma, T. Richeton, S. Dechanel,

F. Louchet, and L. Truskinovsky, Phys. Rev. Lett. **114**, 105504 (2015).
[4] I. Groma, "Statistical physical approach to describe the collective properties of dislocations," in *Multiscale Modelling of Plasticity and Fracture by Means of Dislocation Mechanics* (Springer, New York, 2010) pp. 213–270.
[5] O. U. Salman and L. Truskinovsky, Phys. Rev. Lett. **106**, 175503 (2011).
[6] P. D. Ispánovity, L. Laurson, M. Zaiser, I. Groma, S. Zapperi, and M. J. Alava, Phys. Rev. Lett. **112**, 235501 (2014).
[7] M. Haataja, J. Müller, A. D. Rutenberg, and M. Grant, Phys. Rev. B **65**, 165414 (2002).
[8] K. R. Elder, M. Katakowski, M. Haataja, and M. Grant, Phys. Rev. Lett. **88**, 245701 (2002).
[9] K. R. Elder, N. Provatas, J. Berry, P. Stefanovic, and M. Grant, Phys. Rev. B **75**, 064107 (2007).
[10] V. I. Levitas and M. Javanbakht, Phys. Rev. B **86**, 140101 (2012).
[11] J. Berry, J. Rottler, C. W. Sinclair, and N. Provatas, Phys. Rev. B **92**, 134103 (2015).
[12] D. Taha, S. K. Mkhonta, K. R. Elder, and Z.-F. Huang, Phys. Rev. Lett. **118**, 255501 (2017).
[13] A. D. Rollett, R. Suter, and J. Almer, Annual Review of Materials Research **47** (2017).
[14] R. Suter, Science **356**, 704 (2017).
[15] A. Yau, W. Cha, M. Kanan, G. Stephenson, and A. Ulvestad, Science **356**, 739 (2017).
[16] A. Sarac, M. Oztop, C. Dahlberg, and J. Kysar, International Journal of Plasticity **85**, 110 (2016).
[17] L. L. Bonilla, A. Carpio, C. Gong, and J. H. Warner, Phys. Rev. B **92**, 155417 (2015).
[18] A. Acharya and C. Fressengeas, Int. J. of fracture **174**, 87 (2012).
[19] A. Acharya and C. Fressengeas, in *Differential Geometry and Continuum Mechanics* (Springer, New York, 2015).
[20] Y. Wang, Y. Jin, A. Cuitino, and A. Khachaturyan, Acta materialia **49**, 1847 (2001).
[21] M. Koslowski, A. M. Cuitino, and M. Ortiz, Journal of the Mechanics and Physics of Solids **50**, 2597 (2002).
[22] V. Bulatov and W. Cai, *Computer simulations of dislocations* (Oxford University Press, Oxford, 2006).
[23] M. E. Gurtin, D. Polignone, and J. Viñals, Mathematical Models and Methods in Applied Sciences **6**, 815 (1996).
[24] A. M. Kosevich, in *Dislocations in Solids*, Vol. 1, edited by F. R. N. Nabarro (North-Holland, New York, 1979) p. 33.
[25] D. R. Nelson and J. Toner, Phys. Rev. B **24**, 363 (1981).
[26] J. M. Rickman and J. Viñals, Phil. Mag. A **75**, 1251 (1997).
[27] J. J. Eggleston, G. B. McFadden, and P. W. Voorhees, Physica D: Nonlinear Phenomena **150**, 91 (2001).
[28] K. R. Elder and M. Grant, Phys. Rev. E **70**, 051605 (2004).
[29] K.-A. Wu and P. W. Voorhees, Phys. Rev. B **80**, 125408 (2009).
[30] M. Bjerre, J. M. Tarp, L. Angheluta, and J. Mathiesen, Phys. Rev. E **88**, 020401 (2013).
[31] Z.-F. Huang and K. R. Elder, Phys. Rev. Lett. **101**, 158701 (2008).
[32] P. Y. Chan, G. Tsekenis, J. Dantzig, K. A. Dahmen, and N. Goldenfeld, Phys. Rev. Lett. **105**, 015502 (2010).
[33] J. M. Tarp, L. Angheluta, J. Mathiesen, and N. Goldenfeld, Phys. Rev. Lett. **113**, 265503 (2014).
[34] V. Heinonen, C. V. Achim, K. R. Elder, S. Buyukdagli, and T. Ala-Nissila, Phys. Rev. E **89**, 032411 (2014).
[35] K. Kawasaki and T. Ohta, Physica **139A**, 223 (1986).
[36] R. Tamate, K. Yamada, J. Viñals, and T. Ohta, J. Phys. Soc. Jpn. **73**, 034802 (2008).
[37] P. Martin, O. Parodi, and P. Pershan, Phys. Rev. A **6**, 2401 (1972).
[38] K. R. Elder, Z.-F. Huang, and N. Provatas, Phys. Rev. E **81**, 011602 (2010).
[39] E. D. Siggia and A. Zippelius, Phys. Rev. A **24**, 1036 (1981).
[40] Y. Shiwa and K. Kawasaki, J. Phys. A: Mathematical and General **19**, 1387 (1986).
[41] B. P. Athreya, N. Goldenfeld, and J. A. Dantzig, Phys. Rev. E **74**, 011601 (2006).
[42] D.-H. Yeon, Z.-F. Huang, K. R. Elder, and K. Thornton, Phil. Mag. **90**, 237 (2010).
[43] G. H. Gunaratne, Q. Ouyang, and H. L. Swinney, Phys. Rev. E **50**, 2802 (1994).
[44] B. Halperin, in *Physics of Defects*, edited by R. Balian et al. (North Holland, Amsterdam, 1981).
[45] G. F. Mazenko, Phys. Rev. Lett. **78**, 401 (1997).
[46] G. F. Mazenko, Phys. Rev. E **64**, 016110 (2001).
[47] L. Angheluta, P. Jeraldo, and N. Goldenfeld, Phys. Rev. E **85**, 011153 (2012).
[48] S. M. Cox and P. C. Matthews, Journal of Computational Physics **176**, 430 (2002).
[49] Y. Guo, J. Wang, Z. Wang, J. Li, S. Tang, F. Liu, and Y. Zhou, Phil. Mag. **95**, 973 (2015).
[50] D. Boyer and J. Viñals, Phys. Rev. Lett. **89**, 055501 (2002).